

Disposable flow cytometer with high efficiency in particle counting and sizing using an optofluidic lens

Chaolong Song, Trung-Dung Luong, Tian Fook Kong, Nam-Trung Nguyen,* and Anand Krishna Asundi

School of Mechanical and Aerospace Engineering, Nanyang Technological University,
50 Nanyang Avenue, Singapore 639798, Singapore

*Corresponding author: mntnguyen@ntu.edu.sg

Received December 16, 2010; revised January 13, 2011; accepted January 21, 2011;
posted February 1, 2011 (Doc. ID 139545); published February 18, 2011

Flow cytometers are widely applied to environmental monitoring, industrial testing, and biochemical studies. Integrating a flow cytometer into microfluidic networks helps to miniaturize the system and make it portable for field use. The integration of optical components, such as lenses, further improves the compactness and thus has been intensively studied recently. However, the current designs suffer from severe light scattering due to the roughness of the solid-based lens interface. In this Letter, we propose a flow cytometer using an optofluidic lens to focus the light beam. Benefiting from the smooth liquid-liquid interface and the refractive-index matching liquid as cladding streams, a light beam can be well focused without scattering. The variations of the signal peak values are reduced, owing to the small beam width at the beam waist. The device presents an efficient and accurate performance on both the counting and sizing of particles. © 2011 Optical Society of America

OCIS codes: 230.3990, 230.4685, 050.1965, 080.3620.

A flow cytometer provides an efficient way for the detection of suspended microparticles or biological cells and the analysis of their physical and chemical properties. The applications of cytometers can be widely found in environmental monitoring [1], industrial testing [2], and clinical analysis [3]. Generally, the suspended particles are directed by a streaming flow to pass through a light beam. The scattering or fluorescent light can be collected by optoelectronic systems and transformed into an electric signal. The interpretation of the signal reveals the biochemical and physical characteristics of the particles. Recently, many efforts have been devoted to integrate the flow cytometer into a microfluidic system. The integration allows the miniaturization of the whole system and makes it portable for field use. Another advantage is that the microfluidic system possesses the ability to easily align the particles into a single line by hydrodynamic focusing using sheath flows. This alignment is critical during the analysis because clogging or agglomerating of particles would result in a misinterpretation.

To further improve the level of integration of the system, optical fiber, which can be inserted into the microfluidic networks, was used to perform both excitation and collection of light instead of using external bulky objectives [4,5]. The problem of merely using optical fiber for excitation includes the low intensity in illumination and inaccuracy in detection owing to the divergent light beam emitted from the fiber. Therefore, some on-chip lenses have been proposed to focus the light beam from the fiber. Wang *et al.* designed a flow cytometer with a polydimethylsiloxane (PDMS)-based lens [6] and Godin *et al.* demonstrated a fluidic lens for flow cytometry [7]. Barat *et al.* built a waveguide and lens that were both based on a polymer for a flow cytometer [8]. However, due to the solid-based lens interfaces, all of these designs suffer from light scattering, which degrades the quality of the focused light beam. Divergence or scattering of the light beam results in a larger beam width. An obvious disadvantage resulting from the large beam width is that the cytometer would miscount if multiple particles enter the large illumination area. This is because the multiple

particles would give only one burst in the collected signal. Normally, this burst owing to multiple particles has a larger peak value than one particle. Thus, the other consequent problem is that the signal burst would be misleading, as it would be wrongly interpreted as a larger particle.

Therefore, a well-focused, nonscattered light beam is highly demanded for improving the efficiency and accuracy of a microfluidic flow cytometer. Recently, optofluidic lenses, such as convex [9] and concave [10] geometries, have been proposed to perform light focusing in microfluidic systems. In this Letter, we design a microfluidic flow cytometer with an optofluidic lens formed in a circular chamber. This optofluidic lens has a mathematically predictable focal length and is immune to light scattering [11,12]. A well-focused light beam is achieved with a much smaller beam width of $23\ \mu\text{m}$ compared to all previous flow cytometers. This flow cytometer presents a good performance on particle counting, and the signal intensities shows small aberrations and strong dependence on the particle size.

Figure 1 illustrates the schematic configuration of the flow cytometer integrated into a microfluidic network. The device was fabricated in PDMS with standard soft lithography technique and a channel depth of $150\ \mu\text{m}$. A predefined channel was positioned along the optical

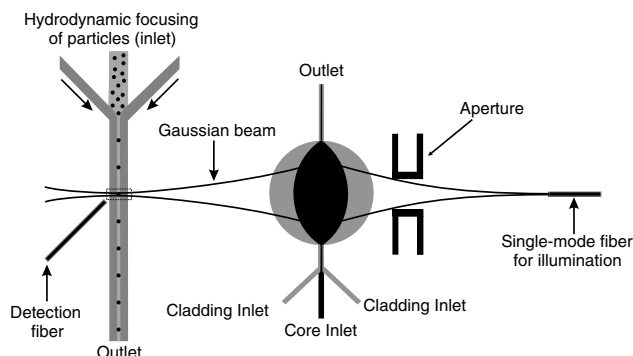


Fig. 1. Schematic configuration of a microfluidic flow cytometer using an optofluidic lens.

axis for introducing a single-mode fiber (SMF), whose tip was at a distance of 4 mm from the center of the optofluidic lens. Two symmetric channels filled with ink acted as the aperture with a width of $350\ \mu\text{m}$. A liquid-core liquid-cladding optofluidic lens was developed in the circular chamber with a diameter of 1 mm to focus the diverging Gaussian beam emitted from the fiber tip. Another fluidic channel with a width of $300\ \mu\text{m}$ was built for hydrodynamic focusing of the particles. The center of this channel was at a distance of 4 mm from the lens. The light scattered by the flowing particle was collected by a multimode fiber (AFS105/125Y, Thorlabs, Inc.) placed with an angle of 45° to the optical axis. The optical signal was transferred to an avalanche photodiode module (C5460-01, Hamamatsu Phototonics, Japan) to generate the electric signal that was recorded by an oscilloscope (Tektronix TDS320) connected to a personal computer.

A preliminary test was carried out to optimize the Gaussian beam profile along the channel where particles flow. In the optimization, a flow-rate ratio ($\phi_{\text{core}}/\phi_{\text{cladding}}$) between core and cladding streams of 6 was chosen to form the optofluidic lens [Fig. 2(b)]. In the experiment, cinnamaldehyde (Sigma Aldrich, USA) with a viscosity of $\mu = 5.7 \times 10^{-3}\ \text{Ns/m}^2$ at 25°C and a refractive index of $n = 1.62$, serves as the core stream to shape the lens. A mixture of 73.5% ethylene glycol and 26.5% ethanol by weight with a viscosity of $\mu = 9.8 \times 10^{-3}\ \text{Ns/m}^2$ at 25°C and refractive index of $n = 1.412$ matching that of PDMS was used as the cladding stream. The significance of the refractive-index matching liquid is the effective prevention of the light beam from scattering, which was explained in detail in our previous works [12,13]. Fluorescence dye, Rhodamine B (Sigma Aldrich, excitation wavelength of 540 nm, emission wave length of 625 nm), that was diluted in a mixture of glycerol (60% by weight) and water (40% by weight) and has a matching refractive index of $n = 1.412$, was injected into the channel for particle focusing to visualize the beam profile. Figure 2 shows the intensity profile extracted along the center line [blue line depicted in the inset 2(a)]. The experimental data can be well-fitted to a Gaussian curve, whose FWHM is defined as the beam width. Under the

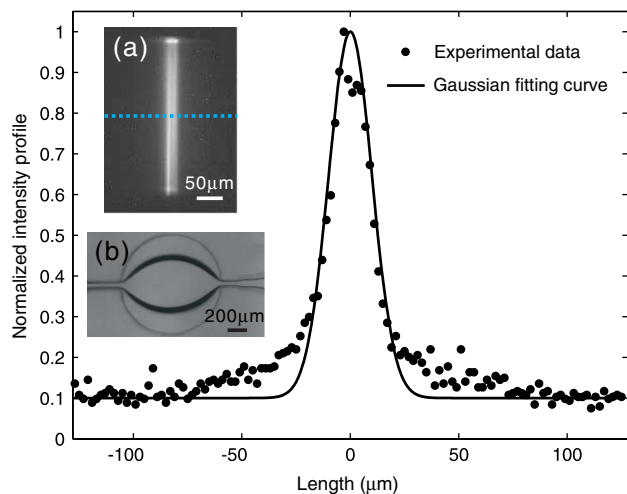


Fig. 2. Intensity profile across the beam waist. (a) Well-focused Gaussian beam across the channel. (b) Optofluidic lens with a flow-rate ratio ($\phi_{\text{core}}/\phi_{\text{cladding}}$) of 6.

optimized condition, the beam width along the center line of the channel can achieve $23\ \mu\text{m}$.

Polymer microspheres of three different sizes were used in the experiment: $20\ \mu\text{m}$ (concentration, $C = 8.6 \times 10^4/\text{ml}$; standard deviation, $0.28\ \mu\text{m}$), $10\ \mu\text{m}$ (concentration, $C = 1.9 \times 10^5/\text{ml}$; standard deviation, $0.09\ \mu\text{m}$), and $5\ \mu\text{m}$ (concentration, $C = 2.8 \times 10^5/\text{ml}$; standard deviation, $0.05\ \mu\text{m}$). The particles were diluted in the mixture of glycerol (60% by weight) and water (40% by weight) with a refractive-index matching of PDMS. This mixture was also used as cladding streams to hydrodynamically focus the particles (1). During the experiment, a flow-rate ratio between core ($50\ \mu\text{l/h}$) and cladding ($500\ \mu\text{l/h}$) streams of 0.1 was chosen to properly align the particles along the center line of the channel. A flow-rate ratio of 6 was used for the optimized lens shape for the detection of particles. When the illuminated space was free of particles, the light beam propagated without scattering, and the detection fiber with an angle of 45° to the optical axis received no light signal. When a flowing particle entered the illuminated space, the mismatch in the refractive index between polystyrene ($n = 1.59$) and liquid ($n = 1.41$) caused the light to refract and reflect. Because of the movement of the particle, the light refraction and reflection was changed, resulting in dynamic scattering of light. Part of the scattered light enters the detection fiber leading to a peak in the signal (Fig. 3). Each peak in Fig. 3 represents a particle passing by, which is the basic concept of particle counting.

The scattered light signals for different sizes of particles are plotted as histograms of peak values [Fig. 4(a)]. The diagram shows separated distributions of the signal peak values for each size of the particle, that indicates small variations of the scattered light signals. The coefficients of variation (CVs), defined as the standard deviation divided by the signal mean value, are 25%,

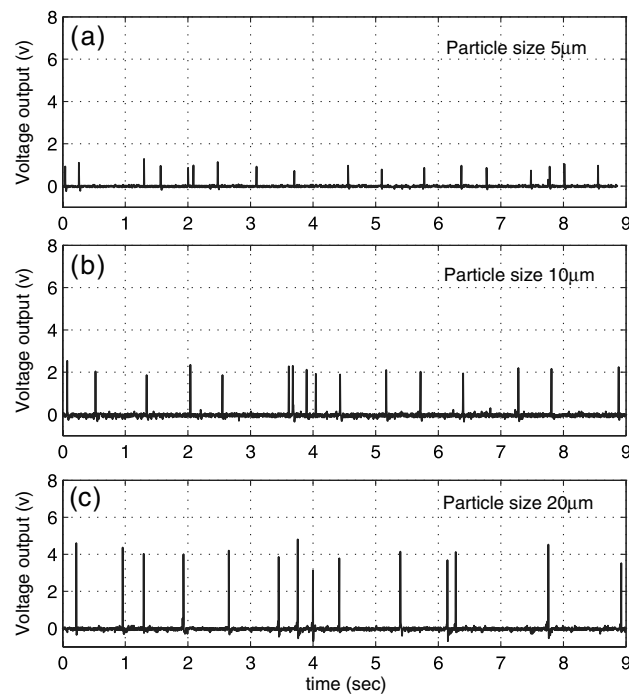


Fig. 3. Scattered light signals for three different sizes of the microsphere: (a) $20\ \mu\text{m}$, (b) $10\ \mu\text{m}$, (c) $5\ \mu\text{m}$.

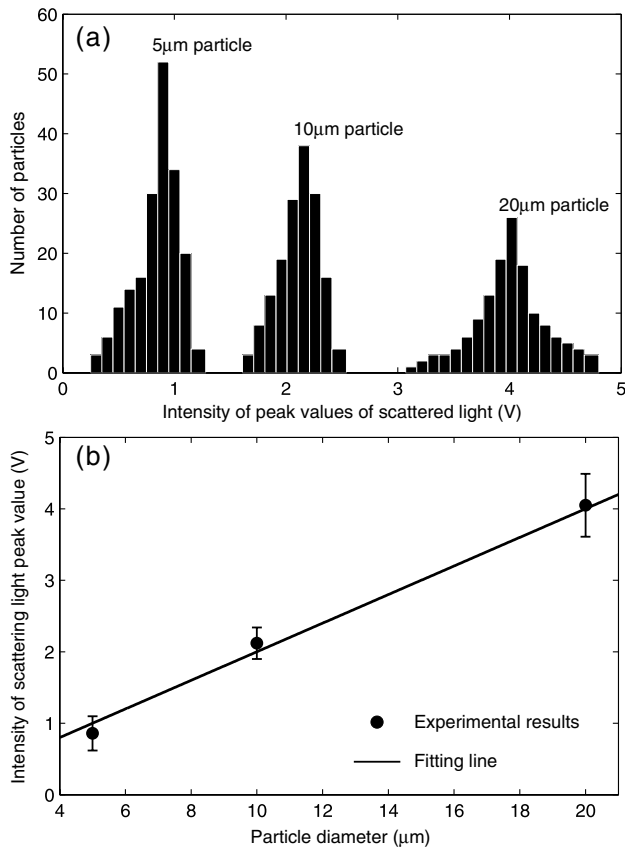


Fig. 4. (a) Distributions of scattered light intensities (peak values) for three different particle sizes. (b) Scattered light intensities as a function of particle sizes.

10%, and 11% for 5, 10, and 20 μm particles, respectively. Under the condition of a small illuminated volume (small beam width at the beam waist), the particles passed through the illuminated space one by one, and the situation of multiple particles simultaneously entering that space was prevented. Multiple particles entering would bring about a larger peak than a single particle. Another reason is that a well-focused and nonscattered light beam helps to increase the intensity of illumination and therefore improve the signal-noise ratio of the light received by the detection fiber. Figure 4(b) shows the scattered light intensity as a function of particle size. Basically, a larger particle has a larger surface to interact with the incident light, and thus results in stronger scattered light to be received by the detection fiber. Achieving lower CVs using our flow cytometer can help to identify the size of the particle more accurately than other previously reported on-chip cytometers [6,7]. However, the CV is

still considered high compared to commercial flow cytometers, especially when the particle size is much smaller than the beam width (the experimental CV of a 5 μm particle is 25%). Although, in this work, we achieved a focused light beam with a beam waist of 23 μm , by using higher refractive-index liquid to develop the optofluidic lens, we can foresee a more tightly focused beam and a narrower beam waist, and a better performance of the microchip flow cytometer.

In conclusion, this Letter presents and demonstrates a disposable and cost-efficient flow cytometer with integrated optical components, such as lens and optical fibers, instead of using external bulky optics. Owing to the well-focused and nonscattered light beam benefiting from the optofluidic lens, the flow cytometer shows a more efficient and accurate performance on particle counting and sizing than previous on-chip flow cytometers [6]. Liquids with refractive-index matching that of PDMS are used for both cladding streams of the optofluidic lens and hydrodynamic focusing of the particle, which is critical for protecting the light beam from being scattered by rough solid interfaces. Using an SMF is another important factor to achieve a small width of the beam waist in the imaged space due to the small core diameter of the SMF ($\sim 5 \mu\text{m}$).

References

1. D. Marie, F. Partensky, S. Jacquet, and D. Vaultot, *Appl. Environ. Microbiol.* **63**, 186 (1997).
2. J. L. Garcia-Cordero, L. M. Barrett, R. O'Kennedy, and A. J. Ricco, *Biomed. Microdevices* **12**, 1051 (2010).
3. C. Alt, I. Veilleux, H. Lee, C. M. Pitsillides, D. Cote, and C. P. Lin, *Opt. Lett.* **32**, 3450 (2007).
4. Y. C. Tung, M. Zhang, C. T. Lin, K. Kurabayashi, and S. J. Skerlos, *Sens. Actuators* **98**, 356 (2004).
5. N. Pamme, R. Koyama, and A. Manz, *Lab Chip* **3**, 187 (2003).
6. Z. Wang, J. El-Ali, M. Engelund, T. Gotsæt, I. R. Perch-Nielsen, K. B. Mogensen, D. Snakenborg, J. P. Kutter, and A. Wolff, *Lab Chip* **4**, 372 (2004).
7. J. Godin, V. Lien, and Y. H. Lo, *Appl. Phys. Lett.* **89**, 061106 (2006).
8. D. Barat, G. Benazzi, M. C. Mowlem, J. M. Ruano, and H. Morgan, *Opt. Commun.* **283**, 1987 (2010).
9. S. K. Y. Tang, C. A. Stan, and G. M. Whitesides, *Lab Chip* **8**, 395 (2008).
10. C. L. Song, N. T. Nguyen, A. K. Asundi, and C. L. N. Low, *Opt. Lett.* **34**, 3622 (2009).
11. C. Song, N. T. Nguyen, S. H. Tan, and A. K. Asundi, *Lab Chip* **9**, 1178 (2009).
12. C. Song, N. T. Nguyen, S. H. Tan, and A. K. Asundi, *Microfluid. Nanofluid.* **9**, 889 (2010).
13. C. Song, N. T. Nguyen, Y. F. Yap, T. D. Luong, and A. K. Asundi, *Microfluid. Nanofluid.* (to be published).